Acta Mechanica Solida Sinica, Vol. 17, No. 4, December, 2004 ISSN 0894-9166
Published by AMSS Press, Wuhan, China. DOI: 10.1007/s10338-004-0439-2

STRESS ANALYSIS AND GEOMETRICAL CONFIGURATION SELECTION FOR MULTILAYER PIEZOELECTRIC DISPLACEMENT ACTUATOR†

Qiu Wei[1] **Kang Yilan**[*1] **Sun Qingchi**[2] **Qin Qinghua**[1] **Lin Yu**[1]
([1]*Department of Mechanics, Tianjin University, Tianjin* 300072*, China*)
([2]*Department of Material Engineering, Tianjin University, Tianjin* 300072*, China*)

Received 18 July 2003; revision received 15 April 2004

ABSTRACT Multilayer piezoelectric ceramic displacement actuators are susceptible to cracking in the region near the edge of the internal electrode, which may cause system damage or failure. In this paper, the stress distribution of a multilayer piezoelectric composite is investigated in a working environment and the optimized geometrical configuration of the piezoelectric layer is obtained. The stress distribution in the structure and the stress concentration near the edge of the internal electrode, induced by non-uniform electric field distribution, are analyzed by moiré interferometry experiment and finite element numerical simulation. Based on the above analysis, two optimized geometrical models are presented for the purpose of geometrical configuration selection, with which stress concentration can be reduced significantly while the feasibility of the machining process and the basic structural functions occurring in the conventional model are retained. The numerical results indicate that the maximum stress in the optimized models is effectively diminished compared to the conventional model. For instance, the peak value of the principal stress in the optimized model II is 93.1% smaller than that in the conventional model. It is proved that stress concentration can be effectively relaxed in the latter of the two optimized models and thus the probability of fracture damage can be decreased.

KEY WORDS piezoelectric multilayer structure, strength analysis, optimized model

I. INTRODUCTION

The multilayer piezoelectric ceramic displacement actuator[1,2] is an important component in intelligent systems and has wide application in laser systems of the space industry. The design of such multilayer piezoelectric actuators is usually based on the principle of electrostriction[2,3]. By electrostriction[3], we mean that a dielectric ceramic expands in the direction of the field and contracts in the direction transverse to the field. As a result, the strains vary approximately with the electric field squared. For such a structure, fracture often occurs near the internal electrode layer and cracks are always initiated at the edge of the electrode when it is in service[3,4]. This may lead to functional invalidation[3,4] or significantly reduce the structural stability, reliability and universality of use[1,5]. Therefore, it is important to study the mechanisms of fracture and stress concentration, to enhance strength and reliability designing for such structures.

During the past decades, studies of interfacial fracture and reliability in multilayer piezoelectric actuators have received considerable attention from researchers and scientists. Winzer et al.[1] analyzed

* Corresponding author, Tel:+86-22-87894001, Fax:+86-22-87894001, E-mail:ylkang@public.tpt.tj.cn
† Project supported by the National Natural Sciences Foundation of China (No.10232030).

the reliability of multilayer electrostrictive actuators. Suo et al.[4] studied the problem of interfacial electric invalidation in piezoelectric bimaterials. Yang and Suo[3] then discussed the stress concentration and electric field distribution theoretically and numerically. Beom and Atluri[6] presented near-tip fields for piezoelectric bimaterials, and Shen et al.[7] and Gao and Wang[8] analyzed the fracture behavior of interfacial crack in a piezoelectric bimaterial. More recently, Qin[9], Qin and Mai[10], Qin and Yu[11] and Yu et al.[12, 13] have reported various crack problems in piezoelectric composites. Fang et al.[14] conducted a series of experiments for testing fracture toughness of certain ferroelectric ceramics. Futakuchi et al.[15] and Zhu et al.[16] presented an approach called the screen-printing method which can be used in structurally optimized design of multilayer piezoelectric structures. However, this method is not suitable for practical design, owing to its lack of feasibility and expense. From the brief review above, it can be noted that most of the existing work is concerned with theoretical models and some specific loading conditions only. There is a lack of investigation of strength analysis and optimized design, and of damage induced by stress concentration of practical multilayer piezoelectric in a working environment. This is the motivation for this paper.

In this paper, a practical structural model of a multilayer piezoelectric ceramic displacement actuator[17] is analyzed numerically and experimentally. The reliability and strength of the multilayer structure are investigated using moiré interference experiments[18−−20] and finite element numerical simulation[21]. Additionally, optimization of the geometry of the piezoelectric layer is performed to obtain optimum stress distribution and thus improve the strength and reliability performance of the structure. Consequently, two improved models are presented with which stress concentration can be significantly reduced while the feasibility of the machining process and the basic structure and functions are retained. The performance of the improved models is compared with the conventional model and numerical assessment is presented at the end of the paper.

II. MULTILAYER PIEZOELECTRIC STRUCTURE AND ITS MODELS

The models used in the analysis are illustrated in Fig.1. These models are presented by considering the practical structural features and working environment. Fig.1(a) shows the conventional model that is composed of shunt-wound piezoelectric layers and thin argent electrodes. The electrodes are distinguished into external and internal ones. On the interface between any two layers there is an electric gap from the edge of the internal electrode to the interface of the external electrode. Owing to the presence of this gap, the two polar electrodes (even the whole structure) can be free of short circuits. However, fracture usually occurs near the tip of the electric gap and the edge of the internal electrode when the structure is in service, i.e., in the working environment. To overcome these shortcomings, two geometrical optimized models (shown in Figs.1(b) and 1(c)) are presented based on finite element modeling and experimental observation. In our analysis, these three models are subjected to various external loads. In particular, two typical loads are considered, firstly the so-called positive loading, for which an electric field is applied on each layer in the poling direction, and secondly negative loading. The magnitude of the electric loading is 4000 kV/m in the positive loading condition and −1000 kV/m in the negative loading condition. The piezoceramic used in this study is plumbic-zirconate-titanate ceramic $[Pb(Zr_{x(0.50\leq x\leq 0.54)}Ti_{1-x})O_3]$ or PZT for short, which is a transversely isotropic material. The geometrical dimensions of the specimens are listed in Table 1 and the material constants of PZT are given in Table 2.

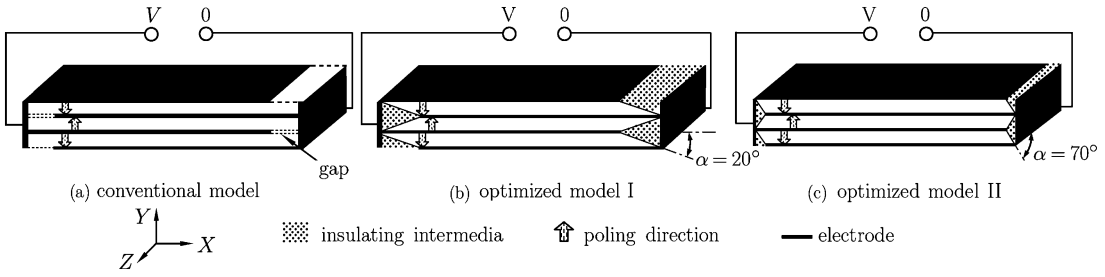

Fig. 1. Schematic illustration of conventional model and optimized models of multilayer piezoelectric structure.

Table 1. **Geometrical dimensions of structure models and specimens**

	length (mm)	width (mm)	height (mm)	thickness per layer (mm)
conventional model	20.34	7.40	2.31	0.77
optimized model I	20.00	7.40	2.31	0.77
optimized model II	18.24	7.40	2.31	0.77
electrode	17.88	7.40	2.31	0.77

Table 2. **Material constants**

elastic compliance (10^{-12} m^2/N)					piezoelectric strain constants (10^{-12} C/N)			dielectric constants ($K_0^\sigma = 8.85 \times 10^{-12}$ F/m)	
s_{11}^E	s_{12}^E	s_{13}^E	s_{33}^E	s_{44}^E	d_{31}	d_{33}	d_{15}	K_{11}^σ/K_0^σ	K_{33}^σ/K_0^σ
16.4	−5.78	7.5	18.8	50	−190	430	730	1720	1700

III. EXPERIMENTS AND NUMERICAL SIMULATION

3.1. Experiment

The optical system of moiré interferometry and phase-shift was set up for this work and is shown in Fig.2. It should be mentioned that moiré interferometry is a highly sensitive optical technique using coherent light. In the optical system, a specimen grating is obtained by replicating a diffraction grating onto the specimen surface. The specimen grating will deform along with the specimen's deformation. The coherent laser light beams illuminate the specimen grating obliquely with an incident angle of 49.4°. When the specimen is deformed, two diffracted light beam from the deformed specimen grating will interfere with each other and form a moiré fringe pattern. The moiré fringe pattern is a contour map of displacement and represents the plane displacement field of the specimen in a particular direction, such as displacement V in y-direction (or displacement U in x-direction). The value of V at a point (x, y) can be obtained from the fringe using the relationship $V(x, y) = N_y/(4f_y)$, where N_y is the order of moiré fringes in fringe pattern at the point and f_y is the specimen frequency in y-direction. A value of $4f_y = 2400$ lines/mm was used in this study and thus each fringe represents 0.417 μm displacement. In this study, specimens were required to be airproofed and insulated by silicon rubber before being loaded with high voltage to avoid electric shock. In addition, to study the effect of the magnitude and direction of electric field on stress distribution and stress concentration, the structure was assumed to be loaded by the external electric field only, i.e., no external mechanical loading was applied to the structure in this study. Figure 3 shows the fringe pattern near the edge of the electrode in the conventional model under +4000 kV/m electric field loading.

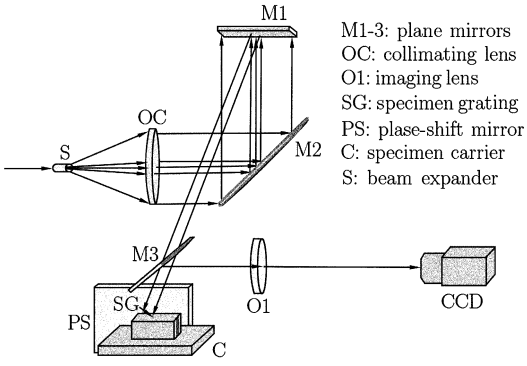

Fig. 2. Small illuminating-field single-beam phase-shift Moiré interferometry optical system.

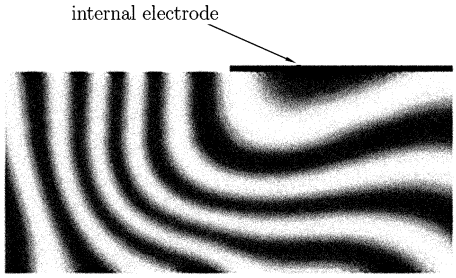

Fig. 3. Fringe pattern near the edge of the internal electrode.

3.2. Numerical Simulation

Numerical simulation was performed using the finite element package ABAQUS (V6.2). The configurations of the three structural models mentioned above were computed for the two loading conditions

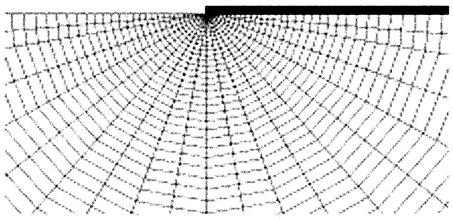

Fig. 4. Finite element mesh near the edge of the electrode.

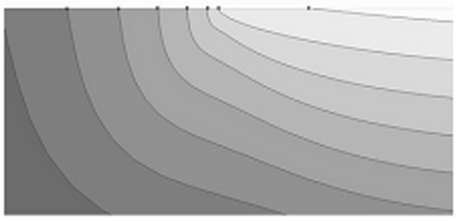

Fig. 5. Displacement contour near the edge of the internal electrode.

(4000 kV/m and −1000 kV/m). In every finite element simulation, more than 5,000 (6,480 in conventional model, 5,717 in optimized model I, 5,303 in optimized model II) four-node plate elements were used. In order to accurately calculate the stress and electric field distributions at the edge of the electrode, the mesh density was increased near the edge of the electrode. The minimal size of the elements near the edge of the internal electrode was 2 μm × 6 μm. A typical finite element mesh near the edge of the electrode is shown in Fig.4. Figure 5 shows the displacement contour obtained from finite element simulation, whose geometry and loading condition are identical to those in Fig.3. It can be seen that the displacement contour shown in Figs. 3 and 5 are quite similar in tendency, which indicates that the results obtained from the two approaches are in good agreement.

IV. RESULTS AND DISCUSSION

As noted by Winzer et al.[1], many microdefects exist in multilayer piezoelectric structures, which may nucleate into various cracks such as interfacial and internal cracks when the structure is in service, leading to interfacial or internal fracture. Interfacial cracks usually occur near the edge or along the electrode layers and are caused by tensile stress or shear stress between piezoceramic layers, whilst internal cracks appear near the edge of the electrode and are caused by tensile stress or shear stress inside the piezoceramic material. The existence of these cracks may cause significant damage or failure of the structure. Therefore, it is important to find ways to relax stress concentration and reduce the maximum stress near the edge of the electrode (enlarged and shown in Fig.6) when the structure is in a working environment. To this end, consider a multilayer piezoelectric structure subject to electrical loading in the y-direction. The electrostrictive strains induced are as follows[9]:

$$(\varepsilon_Z =)\varepsilon_X = d_{31}E_Y, \qquad \varepsilon_Y = d_{33}E_Y \tag{1}$$

where E_Y is the magnitude of the electric field in y-direction; ε_X, and ε_Y are, respectively, the electrostrictive strains in the x- and y-directions, d_{31} and d_{33} are piezoelectric strain constants. It can be seen from Eq.(1) that the electrostrictive strains are determined by both the piezoelectric constants

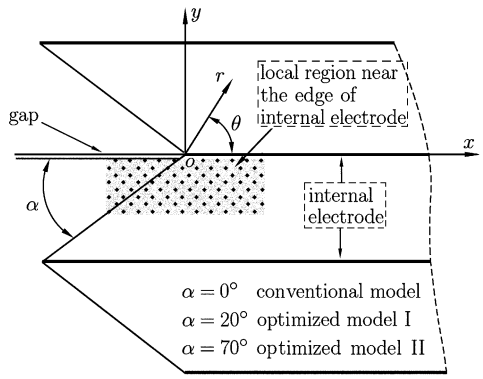

Fig. 6. Enlarged schematic illustration near the edge of the models.

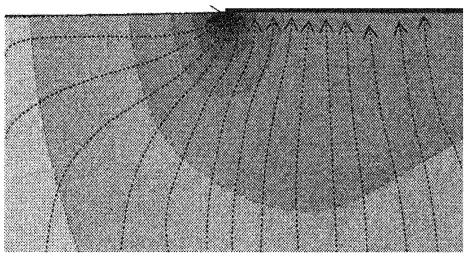

Fig. 7. Distribution of electric field and fluxline near the edge of the internal electrode.

and the applied electric field. The electric field distribution near the edge of the internal electrode is not uniform and is given by[3]

$$\begin{Bmatrix} E_X \\ E_Y \end{Bmatrix} = \frac{K_E}{\sqrt{2\pi r}} \begin{Bmatrix} \cos(\theta/2) \\ \sin(\theta/2) \end{Bmatrix} \tag{2}$$

where K_E is the electric intensity factor; $\sin(\theta/2)$, $\cos(\theta/2)$ are the so-called angle distributing functions of the electric field.

It is necessary to study the features of stress distribution before performing the optimizing process for relaxing maximum stress. It is found from Eq.(2) that the orientation of the electric field near the edge of the internal electrode is the triangular function of polar angle θ. In the front of the electrode edge the orientation is in the direction of the electrode, whilst the orientation of the electric field behind the electrode edge is perpendicular to the electrode. The singularity of the electric field is in the order of minus the square root of distance r. The distribution of the electric field and its flux-line near the electrode edge is shown in Fig.7. It can be seen from the figure that the flux-line becomes dense and the magnitude of the electric field increases rapidly when it approaches the edge of the electrode, indicating that electric field concentration becomes more and more important near the electrode edge.

It should be mentioned that electric field concentration may produce non-uniform electrostriction, which in turn causes non-uniform elastic deformation, because an electric field applied to the piezoelectric layers can induce electrostriction. Such deformation is, however, constrained by the surrounding materials, and consequently leads to non-uniform and incompatible stress, even stress concentration. On the other hand, a relatively high electric field is usually required on the multilayer piezoelectric actuator in order to induce sufficiently large electrostrictive deformation. In this case, very serious stress and electric field concentration may result near the electrode edge for the reason discussed above. Therefore, it is important to determine how to reduce stress concentration using a geometrically optimized model. The finite element simulation below serves this purpose.

The principal stress distribution in the region near the edge of the electrode is shown in Figs.8. It can be seen from the figure that the stress distribution in this region is complicated and stress concentration becomes more important when approaching the electrode edge. Figure 8(a) shows the

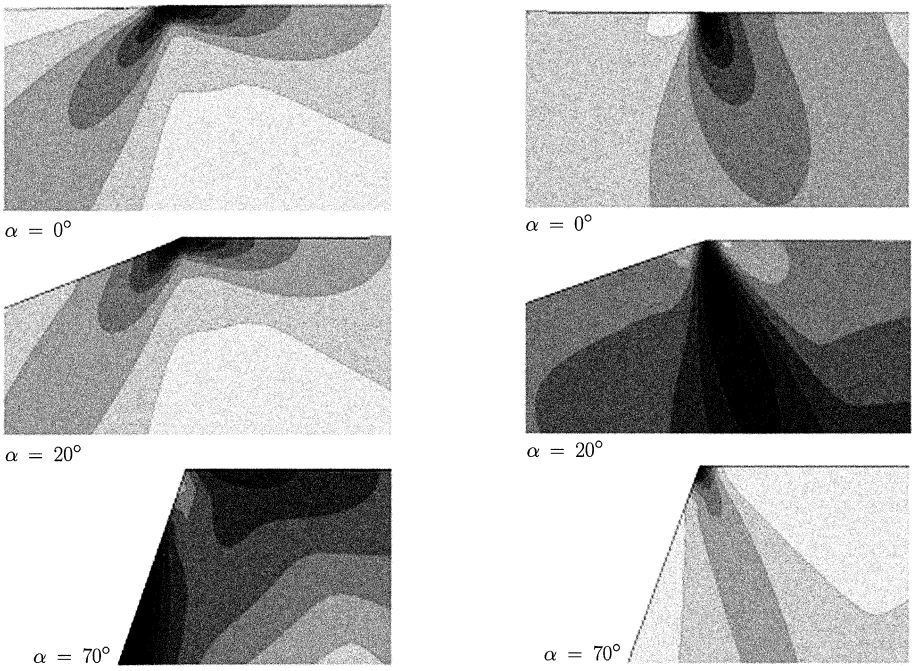

(a) positive loading condition(4000 kV/m) (b) negative loading condition(-1000 kV/m)

Fig. 8. Distribution of principal stress around the gap tip and edge of the internal electrode.

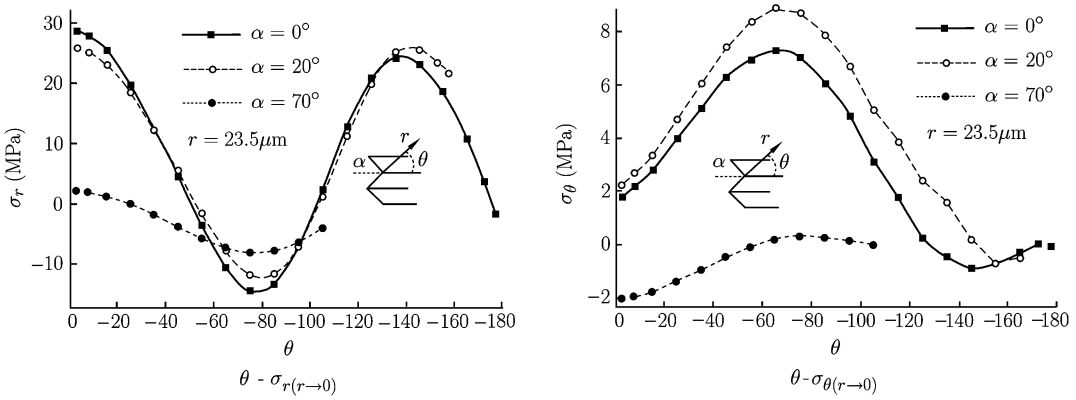

Fig. 9. Curves of $\sigma_{r(r\to 0)}$ and $\sigma_{\theta(r\to 0)}$ near the edge of the internal electrode with positive loading (4000 kV/m).

stress concentration of the conventional model ($\alpha = 0°$) and optimized model I ($\alpha = 20°$) when subject to positive electric load (4000 kV/m). It is evident that stress concentration becomes more and more serious when approaching the electrode edge, and the maximum principal stress can reach 256 MPa at the electrode edge. In contrast, the stress concentration in the optimized model II ($\alpha = 70°$) is reduced remarkably and the maximum principal stress is only about 17 MPa. For the negative electric load (-1000 kV/m), Fig.8(b) presents results of stress distribution similar to those shown in Fig.8(a). It is again shown that the maximum stress in model II (13.7 MPa) is much smaller than that in conventional model (50.2 MPa). To study the difference of stress distribution of σ_r and σ_θ among the three models above, we present the results of σ_r as a function of radial distance r in Fig.9(a), and σ_θ as a function of polar angle θ in Fig.9(b). It is again observed from these two figures that the stress concentration in Model II is significantly reduced in comparison with that in the conventional model.

From the discussion above, it can be seen that the stress concentration and singularity near the electrode edge of the conventional model is obviously serious in the case of both positive and negative electric loads. The stress concentration in model I is little different from that in the conventional model when it is subjected to positive electric load, which indicates that optimized model II is not what we anticipated. However, the stress concentration and the maximum stress in model II can be significantly reduced, and the optimized model II seems to be the best among the three designated models. Some typical results of maximum stress in model II are listed in Table 3 and comparison is made with the conventional model.

Table 3. **Effect of α on maximum stress**

	principal stress (MPa)		shear stress (MPa)		$\sigma_{r(r\to 0)}$ (MPa)		$\sigma_{\theta(r\to 0)}$ (MPa)	
	P*	N*	P	N	P	N	P	N
$\sigma_{\max}$ ($\alpha = 0°$)	256.2	50.2	53.0	7.4	115.1	46.8	194.4	28.9
$\sigma_{\max}$ (α=70°)	17.6	13.7	7.6	1.9	29.6	7.6	29.9	3.8
stress-relaxed degree $(1-\sigma_{\max})/\sigma_{\max}$ ($\alpha = 0°$)	93.1%	72.7%	85.7%	74.3%	74.4%	83.8%	84.6%	86.9%

∗ P: positive loading, N: negative loading.

V. CONCLUSIONS

Stress concentration and fracture mechanism of practical multilayer piezoelectric structure were investigated by experiment and numerical simulation method in this study. The major aspects of this work are as follows:

(1) High stress concentration causing a non-uniform electric field is found near crack tips or the edge of the internal electrode of practical multilayer piezoelectric structures. But the high stress concentration exists in a very small region near the crack tip only and decreases rapidly along with an increase in the distance from the crack tip. The high stress concentration is viewed as the major fracture and damage mechanism of multilayer piezoelectric structures.
(2) Based on experimental analysis and finite element modeling, two geometrical optimized models of multilayer piezoelectric structure have been presented which are proved to be simple and feasible in the manufacturing process without losing any structural functions in comparison with the conventional model. The numerical results obtained from finite element modeling indicate that both stress concentration and the maximum principal stress in the model II ($\alpha = 70°$) can effectively be reduced in comparison with the conventional model ($\alpha = 0°$). In particular, the peak value of the principal stress is 93.1% less than that in the conventional model. The study indicates that the strength and reliability of multilayer piezoelectric structures may be significantly enhanced through use of a geometry optimizing process on the structure.

References

[1] Winzer,S.R., Shankar,N. and Ritter,A., Designing cofired multilayer electrostrictive actuators for reliability, *J. Am. Ceram. Soc.,* Vol.72, 1989, 2246-2257.
[2] Uchino,K., Electrostrictive actuators: materials and application, *Am. Ceram. Soc. Bull.,* Vol.65, 1986, 647-652.
[3] Yang,W. and Suo,Z., Cracking in ceramic actuators caused by electrostriction, *J. Mech. Phys. Solids,* Vol.42, 1994, 649-663.
[4] Suo,Z., Kuo,C.M., Barnett,D.M. and Willis,J.R., Fracture mechanics for piezoelectric ceramics, *J. Mech. Phys. Solids,* Vol.40, 1992, 739-765.
[5] Gong,X. and Suo,Z., Reliability of ceramic multilayer actuators: a nonlinear finite element simulation, *J. Mech. Phys. Solids,* Vol.44, 1996, 751-769.
[6] Beom,H.G. and Atluri,S.N., Near-tip fields and intensity factors for interfacial cracks in dissimilar anisotropic piezoelectric media, *Int. J. Fract.,* Vol.75, 1996, 163-183.
[7] Shen,S.P., Kuang,Z.B. and Hu,S.L., Interface crack problems of a laminated piezoelectric plate, *Eur. J. Mech. A/Solids,* Vol.18, 1999, 219-238.
[8] Gao,C.F. and Wang,M.Z., Green's functions of an interfacial crack between two dissimilar piezoelectric media, *Int. J. Solids Struct.,* Vol.38, 2001, 5323-5334.
[9] Qin,Q.H., Fracture Mechanics of Piezoelectric Materials, Southampton, WIT Press, 2001
[10] Qin,Q.H. and Mai,Y.W., Crack branch in piezoelectric bimaterial system, *Int. J. Engng. Sci.,* Vol.38, 2000, 667-687.
[11] Qin,Q.H. and Yu,S.W., An arbitrarily-oriented plane crack terminating at the interface between dissimilar piezoelectric materials, *Int. J. Solids Struct.,* Vol.34, 1997, 581-590.
[12] Gu,B, Yu,S.W. and Feng,X.Q. et al., Scattering of love waves by an interface crack between a piezoelectric layer and an elastic substrate, *Acta Mech. Solida Sin.,* Vol.15, No.2, 2002, 111-118.
[13] Chen,Z.T. and Yu,S.W., Anti-plane crack moving along the interface of dissimilar piezoelectric materials, *Acta Mech. Solida Sin.,* Vol.12, No.1, 1999, 31-35.
[14] Lu,W., Fang,D.N. and Hwang,K.C., A constitutive theory for ferroelectric ceramics. *Key Engineering Materials,* Vol.145-149, 1998, 983-988.
[15] Futakuchi,T., Yamano,H. and Adachi,M., Preparation of ferroelectric thick film actuator on silicon substrate by screen-printing, *Jpn. J. Appl. Phys. Part 1 Regul. Pap. Short Note Rev. Pap.,* Vol.40, No.9B, 2001, 5687-5689.
[16] Zhu,W., Yao,K. and Zhang,Z., Design and fabrication of a novel piezoelectric multilayer actuator by thick-film screen printing technology, *Sensors and Actuators,* Vol.A86, 2000, 149-153.
[17] Wang,Z.H., Zhu,W.G. and Yao,X., d_{31} type in-plane bending multilayer piezoelectric microactuators – a design concept and its applications, *Sensors and Actuators,* Vol.101, 2002, 262-268.
[18] Post,D., Han,B. and Ifju,P., High sensitivity moiré experimental analysis for mechanics and materials, Berlin, Springer-Verlag, 1994.
[19] Kang,Y.L., Wang,Y.Y. and Jia,Y.Q., New technique of rapid specimen grating making, *Experimental techniques,* Vol.17, 1993, 31-32.
[20] Kang,Y.L. and Wang,S.B. et al., Experimental analysis for singularities in crack normal to bimaterial interface, *Acta Mech. Solida Sin.,* Vol.11, No.2, 1998, 180-186.
[21] Hom,C.L. and Shankar,N., A finite element method for electrostrictive ceramic devices, *Int. J Solids & Structs.,* Vol.33, 1996, 1757-1779.